2000

Reconciliation of the Substorm Onset Determined on the Ground and at the Polar spacecraft

P K. Toivanen

D N. Baker

W K. Peterson

H J. Singer

Niescja E. Turner
Trinity University, nturner1@trinity.edu

See next page for additional authors

GEOPHYSICAL RESEARCH LETTERS, VOL. 28, NO. 1, PAGES 107-110, JANUARY 1, 2001

Reconciliation of the substorm onset determined on the ground and at the Polar spacecraft

P. K. Toivanen [1,7], D. N. Baker [1], W. K. Peterson [2], H. J. Singer [3], N. E. Turner [1], X. Li [1], K. Kauristie [4], M. Syrjäsuo [4], A. Viljanen [4], T. I. Pulkkinen [4] A. Keiling [5], J. R. Wygant [5], and C. A. Kletzing [6]

Abstract.
An isolated substorm on Oct. 17, 1997 during a close conjunction of the Polar spacecraft and the ground-based MIRACLE network is studied in detail. We identify signatures of substorm onset in the plasma sheet midway between the ionosphere and the equatorial plasma sheet, determine their timing relative to the ground signatures, and discuss their counterparts on the ground and in the equatorial plasma sheet. The substorm onset is determined as the negative bay onset at 2040:42(± 5 sec) UT coinciding with the onset of auroral precipitation, energization of plasma sheet electrons at Polar, and strong magnetic field variations perpendicular to the ambient field. Such accurate timing coincidence is consistent with the Alfvén transit time between Polar and the ionosphere. Furthermore, the timing of other field and particle signatures at Polar showed clear deviations from the onset time (± 2 min). This suggests that the sequence of these signatures around the onset time can be used to validate the signatures predicted by various substorm onset models.

1. Introduction

Magnetospheric substorms are global events that are detected by various instruments on the ground and in space. The onset of a substorm is characterized by rapid temporal and spatial changes of plasma and field parameters. The phenomenology and models of the substorm onset are based on well-established signatures, typically deduced from near-equatorial spacecraft or ground-based arrays [e.g., *Baker et al.*, 1996; and *Lui*, 1996]. However, it has not yet been possible to reconcile the time of the substorm onset on the ground and in the equatorial plasma sheet [e.g., *Liou et al.*, 1999; *Ohtani et al.*, 1999]. Thus the cause-and-effect relationship among onset signatures is unclear and this greatly complicates the validation of the substorm onset models.

The Polar spacecraft provides a valuable tool to address the substorm onset in the plasma sheet midway along field lines between the ionosphere and the equatorial plasma sheet. The ISEE-1 spacecraft, for example, also provided observations in this region. *Cattell et al.*, [1982] reported bursty electric fields during substorm activity using ISEE-1 measurements. The state-of-the-art instrumentation onboard Polar provides more complete measurements of various plasma and field parameters with higher time resolution than has previously been available. This is a key requirement for identification and timing of substorm onset signatures.

2. Observations

The event on Oct. 17, 1997 was an isolated substorm. The AE index showed that the substorm onset took place ~ 2041 UT after a quiet period of over two hours. The Wind and Geotail spacecraft were located in the solar wind at $\mathbf{r}_{GSE} \sim$ (65,0,5) R_E and $\mathbf{r}_{GSE} \sim$ (0,-30,0) R_E, respectively. They measured negative IMF $B_{Z_{GSM}}$ before and after the onset. The Los Alamos National Laboratory (LANL) particle sensors onboard a geostationary satellite in the local morning sector recorded two electron injections: at 2047 UT (0342 LT) with energies up to 150 keV; and at 2114 UT (0409 LT) with energies up to 315 keV. An ion injection accompanied the first electron injection in the LANL data.

Ground-based and Polar observations from 2020 UT to 2120 UT are presented in Fig. 1. The north-south (positive toward geographic north) component of the magnetic field variations at the magnetic station of Sørøya (SOR; 67.24 CGM lat., 106.71 CGM long.) (Fig. 1a) indicates a negative bay onset at ~ 2041 UT (vertical line). The westward auroral electrojet was located near SOR: the vertical component (positive downward) at SOR fluctuated around the pre-onset baseline; and the variations in the vertical component were negative (positive) at stations magnetically south (north) of SOR. Occurrence of surge-type variations at nearby stations and a positive eastward component at the lower latitude stations imply that the center of the substorm current wedge was located eastward of the IMAGE chain [*Opgenoorth et al.*, 1983]. The thick horizontal lines along the time axis of Fig. 1a show sequences of magnetic pulsations in the Pi2 range. Fig. 1b shows the intensity of the electron precipitation deduced from the all-sky camera (ASC) at Muonio (MUO; 64.62 CGM lat., 105.70 CGM long.) [*Syrjäsuo et*

[1]Laboratory for Atmospheric and Space Physics, Boulder
[2]Lockheed Martin Space Science Laboratory, Palo Alto
[3]Space Environment Center, NOAA, Boulder
[4]Finnish Meteorological Institute, Helsinki
[5]School of Physics and Astronomy, University of Minnesota, Minneapolis
[6]Department of Physics and Astronomy, University of Iowa, Iowa City
[7]On leave from Finnish Meteorological Institute, Helsinki

Paper number 2000GL000099.
0094-8276/01/2000GL000099$05.00

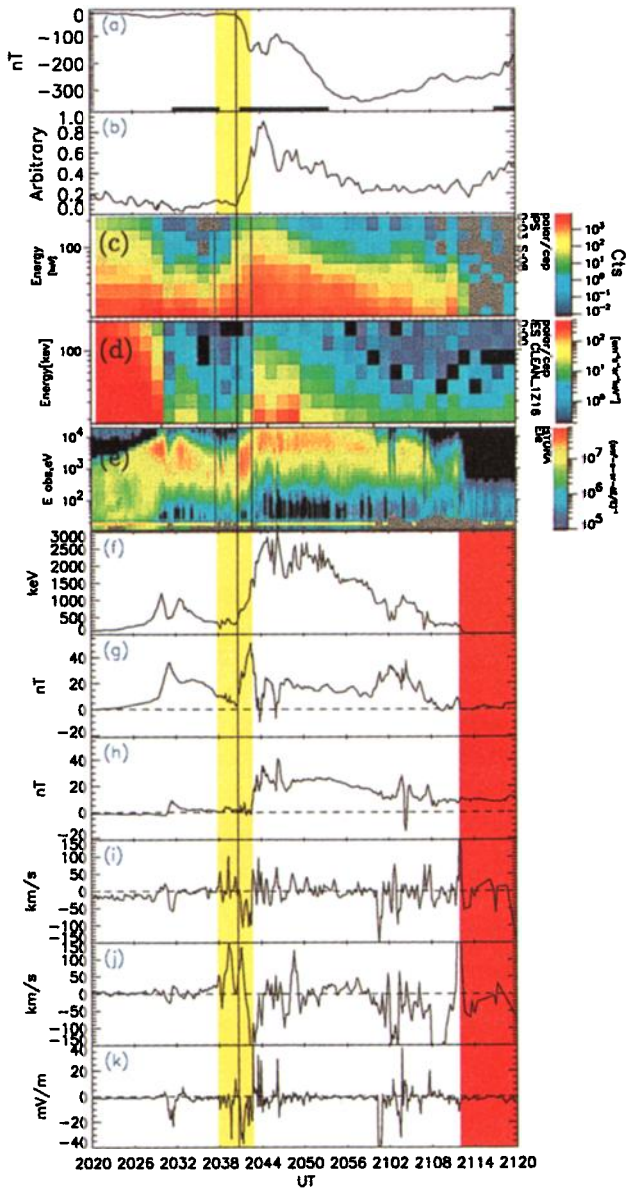

Figure 1. Ground and Polar observations near the substorm onset. The vertical line throughout the panels indicates the substorm onset at 2040:42 UT. The yellow highlights the time range of various onset signatures at Polar. The red shading indicates the tail lobe. The observations shown are: (a) geographic north-south component of the magnetic field variation at SOR; the Pi2 pulsations (the thick lines along the time axis); (b) auroral intensity from station MUO; (c) CEPPAD/IPS proton energy spectrogram; (d) CEPPAD/IES electron energy spectrogram; (e) HYDRA electron energy spectrogram; (f) the mean electron energy determined from HYDRA; (g) Y_{GSM} and (h) Z_{GSM} components of the magnetic field after removal of model field values; (i) Y_{GSM} component of the perpendicular proton flow from TIMAS; (j) magnetic field-aligned proton flow from TIMAS; and (k) Z_{GSE} component of the electric field.

al., 1998]. This was determined from the MUO keogram by integrating intensity of the auroral emission from 100 km south of the station to 100 km north of the station. An abrupt enhancement in electron precipitation at MUO (Fig. 1b) coincided with the negative bay onset. Note that it was cloudy in northern Scandinavia during the event and the auroral activity was captured through the clouds.

During the interval studied, Polar was located in the midnight sector (Table 1; Polar location at the onset). Figs. 1c–1e show energy spectrograms deduced from CEPPAD/IPS (17–235 keV protons), CEPPAD/IES (18–200 keV electrons), and HYDRA (0.01–20 keV electrons) instruments on Polar [*Blake et al.*, 1995; *Scudder et al.*, 1995]. They indicate that Polar was in the plasma sheet prior to and after the onset: the outer radiation belt was seen as high fluxes in CEPPAD/IES before ~ 2029 UT; the plasma sheet was observed by HYDRA between ~ 2025 UT and ~ 2112 UT; the tail lobe appeared as low fluxes in HYDRA after ~ 2112 UT. Prior to the onset, the particle data indicate that Polar was located clearly outside the 40-keV electron trapping boundary and close to the plasma sheet boundary (compare the CEPPAD fluxes at 2040 UT to those observed at ~ 2105 UT).

The field measurements are shown in Figs. 1g–1k. Magnetic field measurements by MFE [*Russell et al., 1995*] are presented as $\delta B_{Y_{GSM}}$ (Fig. 1g) and $\delta B_{Z_{GSM}}$ (Fig. 1h) after the removal of the magnetic field model (see the caption of Table 1) values from the actual measurements. At the onset, the ambient magnetic field was essentially in the X_{GSM} direction, and Y_{GSM} and Z_{GSM} closely represent the coordinates perpendicular to the ambient field. The three bottom panels of Fig. 1 display the proton flow (Figs. 1i and 1j), and electric field (Fig. 1k) measurements. The proton vector velocities were obtained from moments of the three dimensional ion distributions of the TIMAS instrument [*Shelley et al., 1995*]. They are consistent with the electric field measured by the EFI instrument [*Harvey et al.*, 1995]. Prior to the onset, Polar observed a sequence of perpendicular flow bursts (Fig. 1i) and large field-aligned flows (Fig. 1j), caused by proton beams with energies from ~ 3 keV up to the upper energy limit of TIMAS (33 keV). These signatures can be pre-cursors of the onset. Alternatively, they can be associated with the plasma sheet boundary and further support the Polar location near the plasma sheet boundary.

At the onset, an abrupt enhancement in electron fluxes (Fig. 1e) and an increase in the electron mean energy (Fig. 1f) were observed by HYDRA. In CEPPAD/IES, a sudden flux enhancement occurred ~ 2 min later. CEPPAD/IPS measured a more gradual flux increase embedded in the proton background of the plasma sheet. A sudden deviation (~ 40 nT) of the magnetic field from the model field was indicated by $\delta B_{Y_{GSM}}$. After the onset $\delta B_{Y_{GSM}}$ fluctuated with a period of ~ 2.3 minutes. The deviation of the Z_{GSM} component occurred ~ 2 min later. The Y_{GSM} component of the perpendicular flow was reversed ~ 3 min after the first appearance of flow bursts at ~ 2038 UT (Fig. 1i). Note also the dynamical signature at ~ 2030 UT, which has been interpreted as a pseudobreakup by *Peterson et al.*, [2000].

Table 1. Polar location at the onset

UT	Height	MLT	Lat. [a]	Long. [a]	X_{GSM} [b]
2040	4.0 R_E	0015	65.9°	123.1°	-8.3 R_E

[a]Corrected GeoMagnetic coordinates of Polar footpoint as determined from a superposition of the T89 model [*Tsyganenko*, 1989] and the International Geomagnetic Reference Field, IGRF.

[a]Mapping of the Polar field line in the equatorial plasma sheet.

Table 2.

Ground	Polar	Tail
◇ Formation of the auroral electrojet.	◇ Field-aligned currents.	
◇ Precipitation of energetic electrons.	◇ Enhancement in the mean electron energy.	◇ Electron energization.
◇ Onset of broad band Pi2 pulsation	◇ Magnetic field fluctuations in the Pi2 frequency range.	
	◇ Sudden enhancement in $B_{Z_{GSM}}$.	◇ Onset of dipolarization.
	◇ Flux enhancement in energy ranges $\gtrsim$ 75 keV.	◇ Dispersionless particle injection.
	◇ Fast flow bursts and impulsive electric field.	◇ Fast bursty flow with northward B_Z in the near-Earth plasma sheet.

3. Results: Onset at 2040:42 UT

The observations presented in Fig. 1 allow us both to identify several onset signatures at Polar and to determine their timing with respect to the ground signatures. It is important that the onset have taken place in the local time sector covered by Polar and MIRACLE. There are two facts that support this: the westward traveling surge propagates typically 3–5 km/s [*Opgenoorth et al.*, 1983]; and the Polar foot points were clearly east of the stations. Thus if the expansion onset was initiated earlier and further east than Polar, a time lag of 2–3 min should occur between the Polar and SOR data. Furthermore, the good correlation between the rise times of the precipitation at MUO (Fig. 1b) and the mean electron energy at Polar (Fig. 1f) also favor this interpretation.

The particle flux enhancements, in principle, can be a combination of three (spatial/temporal) processes: the first is the plasma sheet expansion, which displaces Polar inward relative to the regions of higher fluxes (spatial); the second is the energization on the Polar field line (temporal); and the third is the drift of energized particle populations to the Polar location (spatial). Any definite separation between these three processes is difficult without an extensive analysis of particle spectra, which is beyond the scope of this paper. However, we anticipate that the observed flux enhancements were mainly caused by plasma sheet expansion and energization. The plasma sheet expansion is apparent as a clearly larger extent of the post-onset plasma sheet (Figs. 1c and 1e). The good agreement between the mean electron energy deduced from HYDRA (Fig. 1f) and the electron precipitation at MUO (Fig. 1b) strongly argues for a temporal flux enhancement. Furthermore, the delay of the flux enhancement in CEPPAD/IES can be attributed to the energization reaching the instrument energy range. Finally, the Polar location in the tail prior to the onset indicates that Polar was unable to see any earthward propagating injection fronts.

Table 2 lists the onset signatures at Polar and their counterparts on the ground and in the tail. Here, we mainly address the relationships between the signatures at Polar and on the ground as no data from the equatorial plane in the onset meridian were used. However, an outline of relationships between Polar and locations in the tail is added for discussion. The electron precipitation and the electron mean energy at Polar showed a strong positive correlation around the onset time. This can further be related to the electron energization in the equatorial plasma sheet. The flux increase measured by CEPPAD may be a signature of the particle acceleration that leads later to the particle injection in the energy ranges $\gtrsim$ 75 keV observed at the geostationary orbit. Part of the flux increase is caused by the plasma sheet expansion. The abrupt deviation of the Y_{GSM} component of the residual magnetic field at the onset can be associated with field-aligned currents and formation of the auroral electrojet. The magnetic fluctuations at Polar occurred in the Pi2 frequency range and can thus be related to the Pi2 pulsations observed on the ground. Thus the field variations are most probably a signature of an Alfvén wave propagating from the tail to the ionosphere. A similar conclusion was also drawn by *Wygant et al.* [2000]. The increase of $\delta B_{Z_{GSM}}$ is a typical signature of dipolarization, but the field-aligned currents significantly contribute to the total magnetic field at Polar altitude. Flow bursts at Polar may be a signature of enhanced flows in the equatorial plasma sheet.

We define the main onset time to be 2040:42 UT±5 sec as the negative bay onset at SOR. Fig. 2 summarizes the

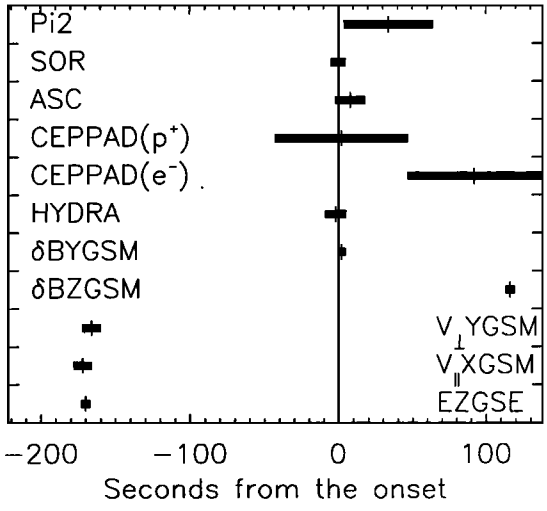

Figure 2. Summary of the onset signatures. The short vertical lines gives the "best guess" of the onset time for each measurements. The black thick lines show the resolution of the corresponding data. The onsets at CEPPAD are derived from the energy channels 103–142 keV (protons) and 75 – 105 keV (electrons) corresponding to the energy channels in which the injections were observed by the LANL spacecraft.

timing of the other signatures relative to the onset. An important feature of the timing is that the onset is simultaneous on the ground and at Polar to within the time resolution of the data. This is reasonable as the Alfvén travel time from Polar to the ionosphere is typically less than 10 sec. Another important aspect of this event is that the timing of several signatures at Polar deviates from the onset, most notably, the flow bursts, the dipolarization, and the flux enhancement of higher energy electrons. This may indicate that the flows in the plasma sheet are enhanced before the dipolarization and electron injection at geostationary distances.

4. Summary and Discussion

We have identified a new previously unreported substorm onset signature in the particle and field measurements midway along field lines between the ionosphere and the equatorial plasma sheet. The event reported was observed by the Polar spacecraft on October 17, 1997. Polar was able to capture the onset of an isolated substorm by entering the plasma sheet prior to, and remaining after, the onset. Furthermore, Polar was in a close conjunction with the ground-based MIRACLE array.

These observations were used to define the substorm onset time and to relate space-based signatures observed at Polar with those observed on the ground (Table 1). The substorm onset at 2040:42($\pm$ 5 sec) UT was defined as the negative bay onset coinciding with the onset of auroral precipitation. The onset signatures of electron energization and field-aligned currents at Polar were simultaneous with the ground onset within the Alfvén transit time between the ionosphere and the Polar altitude ($\lesssim$ 10 sec). The accurate timing of the signatures on the ground and at Polar suggests that the auroral breakup, the negative bay onset, and the initiation of auroral zone Pi2 pulsations are simultaneous signatures for the substorm expansion onset reaching the ionosphere. This naturally requires that the magnetic stations are located near the auroral breakup region [*Rostoker et al.*, 1980].

The results of this paper give confidence to investigate substorm onsets for several more events, especially for those with observations available in the equatorial plasma sheet. In addition to the accurate onset determination, several dynamical features showed timing which deviated clearly from the onset. These deviations from the onset time suggest that not only the field-aligned propagating signatures are detected at Polar, but also features that are more confined in the equatorial plasma sheet can remotely be monitored from the Polar altitude. This encourages similar use of our the data set to test ground truth for models that attempt to solve the problem of substorm onset.

Acknowledgments. This work was supported by grants from the NASA/GGS program. W. K. Peterson thanks the staff at LASP for their hospitality and NASA contract NAS5-30302 for support. H. J. Singer appreciates support from NOAA and the NASA POLAR mission through Interagency Agreement #S-67019-F. The MIRACLE network is operated as an international collaboration under the leadership of the Finnish Meteorological Institute. The IMAGE magnetometer data are collected as a Finnish-German-Norwegian-Polish-Russian-Swedish project. Analysis of electric field data was supported by NASA ISTP (NASA contract NAG 5-3182). The work of C. A. Kletzing was performed under NASA grant number NAG 5 2231 and DARA grant 50 OC 8911 0. The results of the HYDRA investigation were made possible by the decade-long hardware efforts of groups led at NASA GSFC by K. Ogilvie, at UNH by R. Torbert, at MPAe by A. Korth and UCSD by W. Fillius. We are also thankful to C. T. Russell for provision of MFE data and online data providers G. D. Reeves (LANL data), T. Kamei (*AE*-index), and S. Kokubun (Geotail data).

References

Baker, D. N., T. I. Pulkkinen, V. Angelopoulos, W. Baumjohann, and R. L. McPherron, Neutral line model of substorms: Past result and present view, *J. Geophys. Res., 101*, 12,975–13,010, 1996.

Blake, J. B., et al., Comprehensive energetic particle and pitch angle distribution experiment on Polar (CEPPAD), *Space Science Rev., 71*, 531–562, 1995.

Cattell, C. A., M. Kim, R. P. Lin, and F. S. Mozer, Observations of large electric field near the plasma sheet boundary by ISEE-1, *Geophys. Res. Lett., 26*, 425–428, 1982.

Harvey, P, et al., The electric field instrument on the Polar satellite, *Space Science Rev.,71*, 583–596, 1995.

Liou, K., C.-I. Meng, A. T. Y. Lui, P. T. Newell, M. Brittnacher, G. Parks, G. D. Reeves, R. R. Anderson, and K. Yumoto, On relative timing in substorm onset signatures, *J. Geophys. Res., 101*, 22,807–22,817, 1996.

Lui, A. T. Y., Current disruption in the Earth's magnetosphere: Observations and models, *J. Geophys. Res., 101*, 13,067–13,088, 1996.

Ohtani, S., F. Creutzberg, T. Mukai, H. J. Singer, A. T. Y. Lui, M. Nakamura, P. Prikryl, K. Yumoto, and G. Rostoker, Substorm onset timing: The december 31, 1995, event, *J. Geophys. Res., 104*, 22,713–22,727, 1999.

Opgenoorth, H., R. J. Pellinen, W. Baumjohann, E. Nielsen, G. Marklund, and Lars Eliasson, Three-dimensional current flow and particle precipitation in a westward travelling surge (Observed during the Barium-GEOS rocket experiment), *J. Geophys. Res., 88*, 3138–3152, 1983.

Peterson, W. K., P. K. Toivanen, X. Li, D. N. Baker, A. Keiling, J. Wygant, C. A. Kletzing, and C. T. Russell, Polar observations of two pseudobreakup events, *submitted to Proceedings of the International Conference on Substorms-5*, 2000.

Rostoker, G., S.-I. Akasofu, J. Foster, R. A. Greenwald, Y. Kamide, K. Kawasaki, A. T. Y. Lui, R. L. McPherron, and C. T. Russell, Magnetospheric substorms–Definition and signatures, *J. Geophys. Res., 85*, 1663–1668, 1980.

Russell, C. T., et al., The GGS\Polar magnetic fields investigation, *Space Science Rev.,71*, 563–582, 1995.

Scudder, J., et al., HYDRA-A 3-dimensional electron and ion hot plasma instrument for the Polar spacecraft of the GGS mission, *Space Science Rev.,71*, 459–495, 1995.

Shelley, E. G., et al., The toroidal imaging mass-angle spectrograph (TIMAS) for the Polar mission, *Space Science Rev.,71*, 497–530, 1995.

Syrjäsuo, M. T., et al., Observations of substorm electrodynamics using the MIRACLE network, Proceedings of the International Conference on Substorms-4, Editors: S. Kokubun and Y. Kamide, Astrophysics and Space Science Library, vol. 238, Terra Scientific Publishing Company/ Kluwer Academic Publishers, 111–114, 1998.

Tsyganenko, N. A., A magnetospheric magnetic field model with a warped tail current sheet, *Planet. Space Sci., 37*, 5–20, 1989.

Wygant, J. R., et al., Polar spacecraft based comparisons of intense electric fields and Poynting flux near and within the plasma sheet-tail lobe boundary to UVI images: An energy source for aurora, *J. Geophys. Res., 105*, 18,675–18,692, 2000.

P. K. Toivanen, Laboratory for Atmospheric and Space Physics, 1234 Innovation Dr., University of Colorado at Boulder, Boulder, CO 80309. (e-mail: petri.toivanen@lasp.colorado.edu)

(Received May 2, 2000; revised September 6, 2000;
accepted September 20, 2000.)